



# NUMERICAL ANALYSIS OF ARCS IN SUPERSONIC FLOW

C. Bhansali, D.M. Benenson

## ► To cite this version:

C. Bhansali, D.M. Benenson. NUMERICAL ANALYSIS OF ARCS IN SUPERSONIC FLOW. Journal de Physique Colloques, 1979, 40 (C7), pp.C7-263-C7-264. 10.1051/jphyscol:19797129 . jpa-00219101

**HAL Id: jpa-00219101**

**<https://hal.science/jpa-00219101>**

Submitted on 4 Feb 2008

**HAL** is a multi-disciplinary open access archive for the deposit and dissemination of scientific research documents, whether they are published or not. The documents may come from teaching and research institutions in France or abroad, or from public or private research centers.

L'archive ouverte pluridisciplinaire **HAL**, est destinée au dépôt et à la diffusion de documents scientifiques de niveau recherche, publiés ou non, émanant des établissements d'enseignement et de recherche français ou étrangers, des laboratoires publics ou privés.

## NUMERICAL ANALYSIS OF ARCS IN SUPERSONIC FLOW

C.K. Bhansali and D.M. Benenson.

Laboratory for Power and Environmental Studies, Department of Electrical Engineering, State University of New York at Buffalo Amherst, New York, U.S.A.

**Introduction.** The complexities involved in the analysis of an arc immersed in a flowing medium have naturally led to a large number of simplified formulations including (1) the integral method /1/, (2) the one-dimensional approach /2,3/, and (3) two-zone model /4/. The present paper presents the numerical solutions of the coupled, non-linear conservation equations applied to the case of an argon arc within a converging-diverging nozzle and subjected to supersonic flow (in the downstream portion of the nozzle). An ultimate objective is the determination of the behavior of a dynamic plasma as it is current ramped to current zero (and voltage ramped after current zero) - i.e., the circuit interruption problem. The present work describes the steady-state solutions obtained and needed for solution of the dynamic arc. The analysis includes real gas effects, turbulence, and (optically thin) radiation.

**Formulation.** The conservation equations - mass, momentum, and energy - are written, respectively

$$\frac{\partial \rho}{\partial t} + \nabla \cdot (\rho \vec{V}) = 0 \quad (1)$$

$$\frac{\partial (\rho \vec{V})}{\partial t} + \nabla \cdot (\rho \vec{V} \vec{V} - \vec{\tau}) = 0 \quad (2)$$

$$\frac{\partial (\rho e_s)}{\partial t} + \nabla \cdot (\rho e_s \vec{V} + \vec{q} - \vec{V} \cdot \vec{\tau}) = \vec{J} \cdot \vec{E} - Q_r \quad (3)$$

together with the equation of state

$$p = p(\rho, e) \quad (4)$$

and Ohm's law

$$\vec{J} = \sigma \vec{E} \quad (5)$$

(where  $e$  = internal energy,  $e_s = e + \frac{1}{2} V^2$ ,  $\vec{E}$  = electric field,  $\vec{J}$  = current density,  $p$  = pressure,  $\vec{q}$  = heat flux,  $Q_r$  = radiation power density,  $t$  = time,  $\vec{V}$  = velocity,  $\rho$  = density,  $\sigma$  = electrical conductivity,  $\vec{\tau}$  = stress tensor).

Turbulent effects are included through the Prandtl mixing length model with turbulent shear stress given by

$$\tau'_{zr} = \mu_t \frac{\partial u}{\partial r} \quad (6)$$

with

$$\mu_t = \rho \epsilon = \rho c (z - z_t) |U_{\max} - U_{\text{cold}}|$$

and /5/

$$c = 1.4 \times 10^{-4}$$

and turbulent heat flux given by

$$q' = -k_t \frac{\partial T}{\partial r} \quad (7)$$

with

$$k_t = 2\rho C_p c (z - z_t) |U_{\text{cold}}|$$

(where  $C_p$  = specific heat at constant pressure,  $r$  = radial coordinate,  $u$  = axial velocity,  $U_{\text{cold}}$  = axial velocity outside arc,  $U_{\max}$  = axial velocity at centerline,  $z$  = axial coordinate,  $z_t$  = axial location of throat,  $\epsilon$  = eddy diffusivity,  $\mu_t$  = turbulent viscosity).

The arc is placed within the converging-diverging nozzle configuration shown in Fig. 1; axial location  $z = 0$  represents the origin of the plasma.

Experiments are being conducted using a nozzle design similar to that shown in the figure /6/.

Solutions of the governing conservation equations are obtained using a Lax-Wendroff type two step, explicit, second order accurate finite difference method /7/, together with the concept of time splitting. A time dependent approach is employed to solve the steady-state problem (enabling essentially the same numerical procedures to be used with the dynamic, ramped plasma). Starting with assumed initial conditions, the time dependent equations are solved to obtain the steady-state solution as the asymptotic time limit of the non-steady equations. A coordinate transformation is used to transform the converging-diverging nozzle into a circular channel of constant area

$$X = z, Y = r/R(z), t = t' \quad (8)$$

(where  $R(z)$  = nozzle radius).

Further, the equations in the transformed coordinates are written in conservation form

$$\frac{\partial U}{\partial t} + \frac{\partial F}{\partial X} + \frac{\partial G}{\partial Y} + S = 0 \quad (9)$$

where  $U$ ,  $F$ ,  $G$ , and  $S$  are four-dimensional vectors and  $S$  is the source term vector that contains all the terms that are not expressible as derivatives of the independent variables in eqn. (9).

The basic physical inputs are (1) steady-state arc current,  $I = 700$  A and (2) stagnation pressure = 10 atm, which results in an exit pressure of  $\sim 1$  atm. The mass flow is not known a priori and is obtained as part of the solution. In the present case, the argon mass flow,  $\dot{m}$ , is  $\sim 100$  g/s.

**Results.** Axial distributions of centerline temperature,  $T_c$ , and centerline axial velocity  $u_c$ , are shown in Fig. 2. The initial, relatively large temperature and the subsequent reduction with axial location is associated, at least to the throat, with the small initial diameter and the resulting expansion of the column. As seen in the figure, the effect of turbulence is to reduce both the velocity and temperature as compared to the laminar case. The arc diameter,  $D$  is defined through the radial location of, say, the 5000 K isotherm. On this basis and representing the diameter in the form  $D \propto z^m$ , the value of  $m$  is found to be  $\sim 0.5$ . For a nitrogen arc in a converging-diverging nozzle and using (1) a two-zone model /5/,  $m \sim 0.6$  and (2) a one-dimensional model /2/,  $m \sim 0.25$ . Radial distributions of temperature and velocity are given in Figs. 3 and 4, respectively, at two axial locations -  $z = 2.15$  cm (slightly downstream of the throat and  $z = 9.6$  cm (near the exit). The expansion of the column downstream of the throat is clearly evident as is the broad, warm, but not electrically conducting, region near the exit.

## References:

- /1/ M.D. Cowley, "Integral Methods of Analyzing Electric Arcs: I. Formulation," *Journal of Physics D: Applied Physics*, Vol. 17, 1974, pp. 2232-2245.
- /2/ J.J. Lowke and H.C. Ludwig, "A Simple Model for High Current Arcs Stabilized by Forced Convection," *Journal of Applied Physics*, Vol. 46, 1975, pp. 3352-3360.
- /3/ F.R. El-Akkari and D.T. Tuma, "Simulation of Transient and Zero Current Behavior of Arcs Stabilized by Forced Convection," *IEEE Transactions on Power Apparatus and Systems*, Vol. PAS-96, 1977, pp. 1784-1788.
- /4/ W. Hermann and K. Ragaller, "Theoretical Description of the Current Interrupters in HV Gas Blast Breakers," *IEEE Transactions on Power Apparatus and Systems*, Vol. PAS-96, 1977, pp. 1546-1555.
- /5/ W. Hermann and K. Ragaller, "Theoretical U. Kogelschatz, L. Niemeyer, K. Ragaller, and E. Schade, "Experimental and Theoretical Study of a Stationary High-Current Arc in a Supersonic Nozzle Flow," *J. Phys. D: Appl. Phys.*, Vol. 7, 1974, pp. 1703-1722.
- /6/ T. Bernecki, Y.C. Lau, and D.M. Benenson, "Experiments on Arcs in High Speed Flow," State University of New York at Buffalo, Buffalo, New York, in progress.
- /7/ R.W. MacCormack and B.S. Baldwin, "A Numerical Method for Solving the Navier-Stokes Equations with Application to Shock-Boundary Layer Interactions," *AIAA 13th Aerospace Sciences Meeting* Pasadena, California, Paper No. 75-1, 1975.

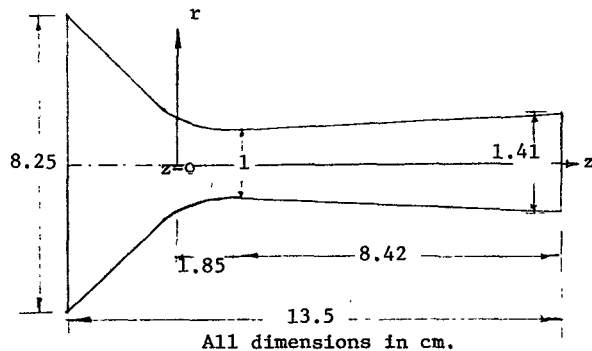


Fig. 1. Nozzle configuration.

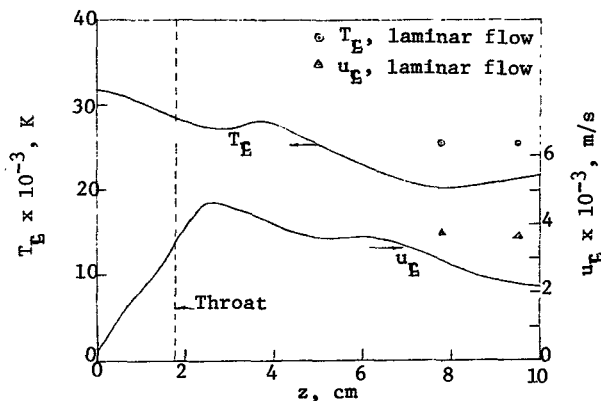
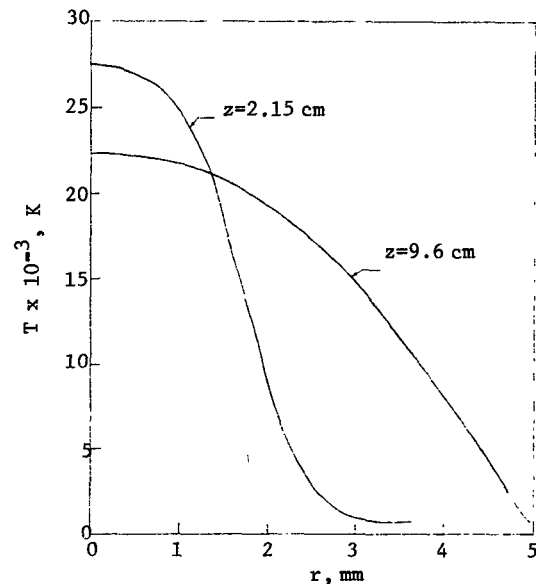
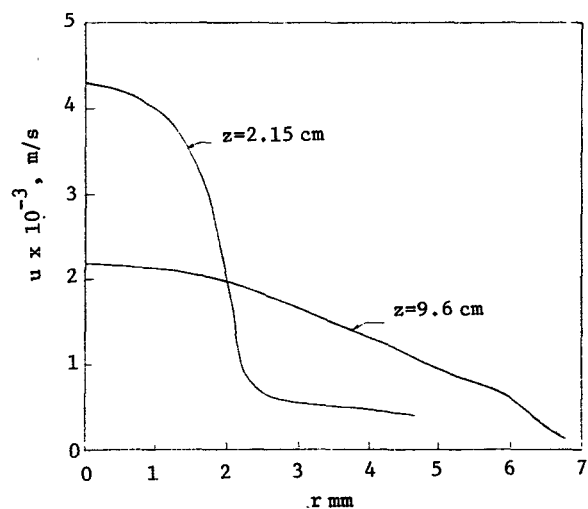


Fig. 2. Axial distributions of centerline temperature and centerline axial velocity.

Fig. 3. Radial distributions of temperature at  $z = 2.15$  and  $9.6$  cm.Fig. 4. Radial distributions of axial velocity at  $z = 2.15$  and  $9.6$  cm.